THE JOURNAL OF PHYSICAL CHEMISTRY LETTERS
A JOURNAL OF THE AMERICAN CHEMICAL SOCIETY

pubs.acs.org/JPCL Letter

Negative Zero-Point-Energy Parameter in the Meyer−Miller Mapping Model for Nonadiabatic Dynamics

Xin He,[†] Zhihao Gong,[†] Baihua Wu, and Jian Liu*

Cite This: J. Phys. Chem. Lett. 2021, 12, 2496−2501 Read Online

ACCESS | Metrics & More | Article Recommendations | Supporting Information

ABSTRACT: The celebrated Meyer−Miller mapping model has been a useful approach for generating practical trajectory-based nonadiabatic dynamics methods. It is generally assumed that the zero-point-energy (ZPE) parameter is positive. The constraint implied in the conventional Meyer−Miller mapping Hamiltonian for an F-electronic-state system actually requires $\gamma \in (-1/F, \infty)$ for the ZPE parameter for each electronic degree of freedom. Both negative and positive values are possible for such a parameter. We first establish a rigorous formulation to construct exact mapping models in the Cartesian phase space when the constraint is applied. When nuclear dynamics is approximated by the linearized semiclassical initial value representation, a negative ZPE parameter could lead to reasonably good performance in describing dynamic behaviors in typical spin-boson models for condensed-phase two-state systems, even at challenging zero temperature.

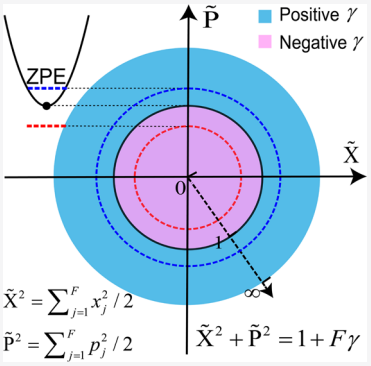

Nonadiabatic processes play an important role when two or more coupled electronic states are involved in complex systems in chemistry, biology, and materials science.[1−3] Of several useful theoretical frameworks for developing practical nonadiabatic dynamics methods, one is the mapping Hamiltonian model proposed in the pioneering work of Meyer and Miller.[4] It maps a coupled F-electronic-state Hamiltonian operator

$$\hat{H} = \sum_{n,m=1}^{F} H_{nm}(\mathbf{R}, \mathbf{P})|n\rangle\langle m| \tag{1}$$

onto a $2F$-dimensional Cartesian phase space $\{\mathbf{x}, \mathbf{p}\} = \{x^{(1)},..., x^{(F)}, p^{(1)},..., p^{(F)}\}$, and yields

$$H_{\mathrm{MM}}(\mathbf{x}, \mathbf{p}; \mathbf{R}, \mathbf{P}) = \frac{1}{2}\mathbf{P}^{\mathrm{T}}\mathbf{M}^{-1}\mathbf{P} + \sum_{n,m=1}^{F}\left[\frac{1}{2}(x^{(n)}x^{(m)} + p^{(n)}p^{(m)}) - \gamma\delta_{nm}\right]V_{nm}(\mathbf{R}) \tag{2}$$

in the diabatic representation, where $\{\mathbf{R}, \mathbf{P}\}$ represents the coordinate and momentum variables for the nuclear degrees of freedom (DOFs) and γ is the parameter accounting for the zero-point energy for each continuous electronic DOF. While $\gamma = 1/2$ in Meyer and Miller's original version,[4] the zero-point-energy (ZPE) parameter is set to $1/3, (\sqrt{3} - 1)/2, (\sqrt{F+1} - 1)/F$, and other non-negative values in its semiclassical/quasiclassical applications.[5−16] Since it is conventionally thought that the zero-point energy should be positive, to the best of our knowledge no negative value has ever been chosen for γ since 1979.

In two alternative approaches, it has been shown that the Meyer−Miller mapping model can be derived in quantum mechanics.[9,17] More interestingly, in the unified framework of phase space mapping models for the (coupled) multistate Hamiltonian (eq 1) in ref 17, the mapping model reminiscent of the Meyer−Miller model reads

$$H_{\mathrm{MM}}(\mathbf{x}, \mathbf{p}; \mathbf{R}, \mathbf{P}) = \sum_{n,m=1}^{F}\left[\frac{1}{2}(x^{(n)}x^{(m)} + p^{(n)}p^{(m)}) - \gamma\delta_{nm}\right]H_{nm}(\mathbf{R}, \mathbf{P}) \tag{3}$$

The comparison between eqs 3 and 2 (for kinetic energy term $\mathbf{P}^{\mathrm{T}}\mathbf{M}^{-1}\mathbf{P}/2$) implies the constraint for the electronic DOFs[15]

$$\mathcal{S}(\mathbf{x}, \mathbf{p}): \sum_{n=1}^{F}\left[\frac{1}{2}((x^{(n)})^2 + (p^{(n)})^2)\right] = 1 + F\gamma \tag{4}$$

Although we use the diabatic representation to reach eq 4, the constraint holds in the adiabatic representation as well. The constraint (eq 4) has already been implied in eqs 43 and 44 of ref 17, and used in ref 15 where $\gamma = 0$ is considered. The physical meaning of eq 4 requires only $\gamma > -1/F$. This confirms that negative values for the ZPE parameter, γ, are possible!

When the underlying mapping DOFs for each (electronic) state are considered to be those of a singly excited oscillator as first suggested in refs 9 and 5, it is natural to view γ as the ZPE parameter for the oscillator. In comparison, the derivation

Received: January 22, 2021
Accepted: February 19, 2021
Published: March 5, 2021

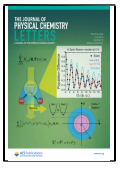

https://dx.doi.org/10.1021/acs.jpclett.1c00232
J. Phys. Chem. Lett. 2021, 12, 2496−2501

procedure of eq 3 in F-dimensional Hilbert space for the electronic DOFs in ref 17 has interpreted the physical concept of parameter γ as a parameter for $\hat{\sigma}_z^{(n)}/2$, where $\hat{\sigma}_z$ is the Pauli spin matrix in the z direction. It has also been clearly stated that parameter γ can be negative.[17]

We first establish the exact mapping with the constraint $\mathcal{S}(\mathbf{x}, \mathbf{p})$ where $\gamma \in (-1/F, \infty)$, with a focus on the F electronic DOFs. In F-dimensional Hilbert space with an orthogonal basis set $\{|\, n = 1,..., F\rangle\}$, the one-to-one correspondence between an operator and its phase space function reads

$$\hat{A} \mapsto A(\mathbf{x},\mathbf{p}) = \mathrm{Tr}_e\left[\hat{A}\hat{K}(\mathbf{x},\mathbf{p})\right] \tag{5}$$

and

$$A(\mathbf{x},\mathbf{p}) \mapsto \hat{A} = \int_{S(\mathbf{x},\mathbf{p})} \mathrm{d}\boldsymbol{\mu}(\mathbf{x},\mathbf{p})\, A(\mathbf{x},\mathbf{p})\hat{K}^{-1}(\mathbf{x},\mathbf{p}) \ , \tag{6}$$

where $\mathrm{Tr}_e[\cdots]$ represents the trace over the F electronic states, $\mathrm{d}\boldsymbol{\mu}(\mathbf{x}, \mathbf{p}) = F\, \mathrm{d}\mathbf{x}\, \mathrm{d}\mathbf{p}$ stands for an invariant measure over the constraint space, $\mathcal{S}(\mathbf{x}, \mathbf{p})$ of eq 4, the kernel is

$$\hat{K}(\mathbf{x}, \mathbf{p}) = \sum_{n,m=1}^{F} \left[\frac{1}{2}(x^{(n)} + ip^{(n)})(x^{(m)} - ip^{(m)}) - \gamma\delta_{nm}\right]|n\rangle\langle m| \tag{7}$$

and the inverse kernel is

$$\hat{K}^{-1}(\mathbf{x}, \mathbf{p}) = \sum_{n,m=1}^{F} \left[\frac{1+F}{2(1+F\gamma)^2}(x^{(n)} + ip^{(n)})(x^{(m)} - ip^{(m)}) - \frac{1-\gamma}{1+F\gamma}\delta_{nm}\right]|n\rangle\langle m| \tag{8}$$

(The derivations of $\hat{K}(\mathbf{x}, \mathbf{p})$ and $\hat{K}^{-1}(\mathbf{x}, \mathbf{p})$ are presented in the Supporting Information.) As expected, the kernel and its inverse are properly normalized

$$\mathrm{Tr}_e[\hat{K}(\mathbf{x}, \mathbf{p})] = \mathrm{Tr}_e[\hat{K}^{-1}(\mathbf{x}, \mathbf{p})] = 1$$
$$\int_{S(\mathbf{x},\mathbf{p})} \mathrm{d}\boldsymbol{\mu}(\mathbf{x}, \mathbf{p})\, \hat{K}(\mathbf{x}, \mathbf{p}) = \int_{S(\mathbf{x},\mathbf{p})} \mathrm{d}\boldsymbol{\mu}(\mathbf{x}, \mathbf{p})\, \hat{K}^{-1}(\mathbf{x}, \mathbf{p}) = \hat{I}_e \tag{9}$$

where $\hat{I}_e$ is the identity operator in F-dimensional Hilbert space for the electronic DOFs. We define the adjoint function in the electronic phase space for operator $\hat{B}$ as

$$\tilde{B}(\mathbf{x}, \mathbf{p}) = \mathrm{Tr}_e[\hat{K}^{-1}(\mathbf{x}, \mathbf{p})\hat{B}] \tag{10}$$

The one-to-one correspondence between the trace of a product of two operators and the overlap integral for the electronic DOFs is then

$$\mathrm{Tr}_e[\hat{A}\hat{B}] = \int_{\mathcal{S}(\mathbf{x},\mathbf{p})} \mathrm{d}\boldsymbol{\mu}(\mathbf{x}, \mathbf{p})\, A(\mathbf{x}, \mathbf{p})\, \tilde{B}(\mathbf{x}, \mathbf{p}) \tag{11}$$

The time correlation function for two operators that involve only the electronic DOFs is

$$C_{AB}(t) = \mathrm{Tr}_e[\hat{A}(0)\hat{B}(t)] = \mathrm{Tr}_e[\hat{A}e^{i\hat{H}t}\hat{B}e^{-i\hat{H}t}] \tag{12}$$

which becomes

$$C_{AB}(t) = \int_{\mathcal{S}(\mathbf{x},\mathbf{p})} \mathrm{d}\boldsymbol{\mu}(\mathbf{x}, \mathbf{p})\, A(\mathbf{x}, \mathbf{p}; 0)\, \tilde{B}(\mathbf{x}, \mathbf{p}; t) \tag{13}$$

i.e., $\hat{A}$ or $\hat{B}$ is replaced by the corresponding Heisenberg operator in eq 11 as well as in eqs 5 and 10. Equation 13 can be evaluated as

$$C_{AB}(t) = \int_{S(\mathbf{x}_0,\mathbf{p}_0)} \mathrm{d}\boldsymbol{\mu}(\mathbf{x}_0, \mathbf{p}_0)\, A(\mathbf{x}_0, \mathbf{p}_0; 0)\, \tilde{B}(\mathbf{x}(t), \mathbf{p}(t); 0)$$
$$= \int_{S(\mathbf{x}_0,\mathbf{p}_0)} \mathrm{d}\boldsymbol{\mu}(\mathbf{x}_0, \mathbf{p}_0)\, A(\mathbf{x}_0, \mathbf{p}_0)\, \tilde{B}(\mathbf{x}_t, \mathbf{p}_t) \tag{14}$$

along trajectory $\{\mathbf{x}(t) \equiv \mathbf{x}_t, \mathbf{p}(t) \equiv \mathbf{p}_t\}$ with initial phase point $\{\mathbf{x}_0, \mathbf{p}_0\}$ at time 0. The equations of motion of the trajectory $\{\mathbf{x}_t, \mathbf{p}_t\}$ are given by the mapping Hamiltonian of eq 3, which is equivalent to solving the time-dependent Schrödinger equation for the electronic DOFs when the nuclear DOFs are frozen.[4,15,17] The mapping formulation (eqs 4−13) for the electronic DOFs is exact in quantum mechanics. Although the Meyer−Miller mapping Hamiltonian is used for demonstration, the mapping formulation can be applied to other mapping models (e.g., those of ref 17). The approach developed in ref 15 is simply a specific case (where $\gamma = 0$) of the formulation.

In nonadiabatic systems, operators $\hat{A}$ and $\hat{B}$ often involve both electronic and nuclear DOFs. The trace operation in eq 12 should then be over both electronic and nuclear DOFs. Equation 13 can be extended as

$$C_{AB}(t) = \mathrm{Tr}_{n,e}[\hat{A}(0)\hat{B}(t)] = \frac{1}{(2\pi\hbar)^N}\int \mathrm{d}\mathbf{R}\, \mathrm{d}\mathbf{P} \int_{S(\mathbf{x},\mathbf{p})} \mathrm{d}\boldsymbol{\mu}(\mathbf{x}, \mathbf{p})\, A_W(\mathbf{R}, \mathbf{P}; \mathbf{x}, \mathbf{p}; 0) \times \tilde{B}_W(\mathbf{R}, \mathbf{P}; \mathbf{x}, \mathbf{p}; t) \tag{15}$$

where the Wigner functions for the nuclear DOFs are

$$A_W(\mathbf{R}, \mathbf{P}; \mathbf{x}, \mathbf{p}) = \int \mathrm{d}\boldsymbol{\Delta} \left\langle \mathbf{R} - \frac{\boldsymbol{\Delta}}{2}\middle| A(\hat{\mathbf{R}}, \hat{\mathbf{P}}; \mathbf{x}, \mathbf{p})\middle| \mathbf{R} + \frac{\boldsymbol{\Delta}}{2}\right\rangle e^{i\boldsymbol{\Delta}\cdot\mathbf{P}/\hbar} \tag{16}$$

and

$$\tilde{B}_W(\mathbf{R}, \mathbf{P}; \mathbf{x}, \mathbf{p}) = \int \mathrm{d}\boldsymbol{\Delta} \left\langle \mathbf{R} - \frac{\boldsymbol{\Delta}}{2}\middle| \tilde{B}(\hat{\mathbf{R}}, \hat{\mathbf{P}}; \mathbf{x}, \mathbf{p})\middle| \mathbf{R} + \frac{\boldsymbol{\Delta}}{2}\right\rangle e^{i\boldsymbol{\Delta}\cdot\mathbf{P}/\hbar} \tag{17}$$

In eq 15, $\int \mathrm{d}\mathbf{R}\, \mathrm{d}\mathbf{P}$ is over the full Wigner phase space for the N nuclear DOFs. On the right-hand side of eq 16 or eq 17 $\{\mathbf{x}, \mathbf{p}\}$ is viewed as parameters.

$A(\hat{\mathbf{R}}, \hat{\mathbf{P}}, \mathbf{x}, \mathbf{p})$ of eq 16 and $\tilde{B}(\hat{\mathbf{R}}, \hat{\mathbf{P}}, \mathbf{x}, \mathbf{p})$ of eq 17 are produced by eq 5 for operator $\hat{A}$ and by eq 10 for operator $\hat{B}$, respectively, only for the electronic DOFs. Equation 15 offers an exact formulation as long as the nuclear dynamics in eq 15 is also exactly solved for the coupled multielectronic-state Hamiltonian in eq 1, regardless of the choice of the ZPE parameter, γ, in domain $(-1/F, \infty)$ for the constraint space (eq 4).

It is often far from trivial to treat the nuclear DOFs in an exact fashion for general nonadiabatic systems. Employing the linearized semiclassical initial value representation (LSC-IVR)/classical Wigner approach to approximate nuclear dynamics,[5] we obtain

$$C_{AB}(t) = \frac{1}{(2\pi\hbar)^N}\int \mathrm{d}\mathbf{R}_0\, \mathrm{d}\mathbf{P}_0 \int_{S(\mathbf{x}_0,\mathbf{p}_0)} \mathrm{d}\boldsymbol{\mu}(\mathbf{x}_0, \mathbf{p}_0)\, A_W(\mathbf{R}_0, \mathbf{P}_0; \mathbf{x}_0, \mathbf{p}_0) \times \tilde{B}_W(\mathbf{R}_t, \mathbf{P}_t; \mathbf{x}_t, \mathbf{p}_t) \tag{18}$$

where trajectory $(\mathbf{R}_t, \mathbf{P}_t; \mathbf{x}_t, \mathbf{p}_t)$ follows classical Hamilton equations of motion yielded by the Meyer−Miller mapping Hamiltonian (eq 2) with initial total phase point $(\mathbf{R}_0, \mathbf{P}_0; \mathbf{x}_0, \mathbf{p}_0)$. The approach is denoted as the extended classical mapping model (eCMM). For instance, consider that the initial total density is $\hat{\rho}_{\mathrm{nuc}} \otimes |n\rangle\langle n|$, where $\hat{\rho}_{\mathrm{nuc}}$ is the initial density operator for the nuclear DOFs and only state $|n\rangle$ is occupied at the beginning. The population of state $|m\rangle$ at time t is

https://dx.doi.org/10.1021/acs.jpclett.1c00232
J. Phys. Chem. Lett. 2021, 12, 2496−2501

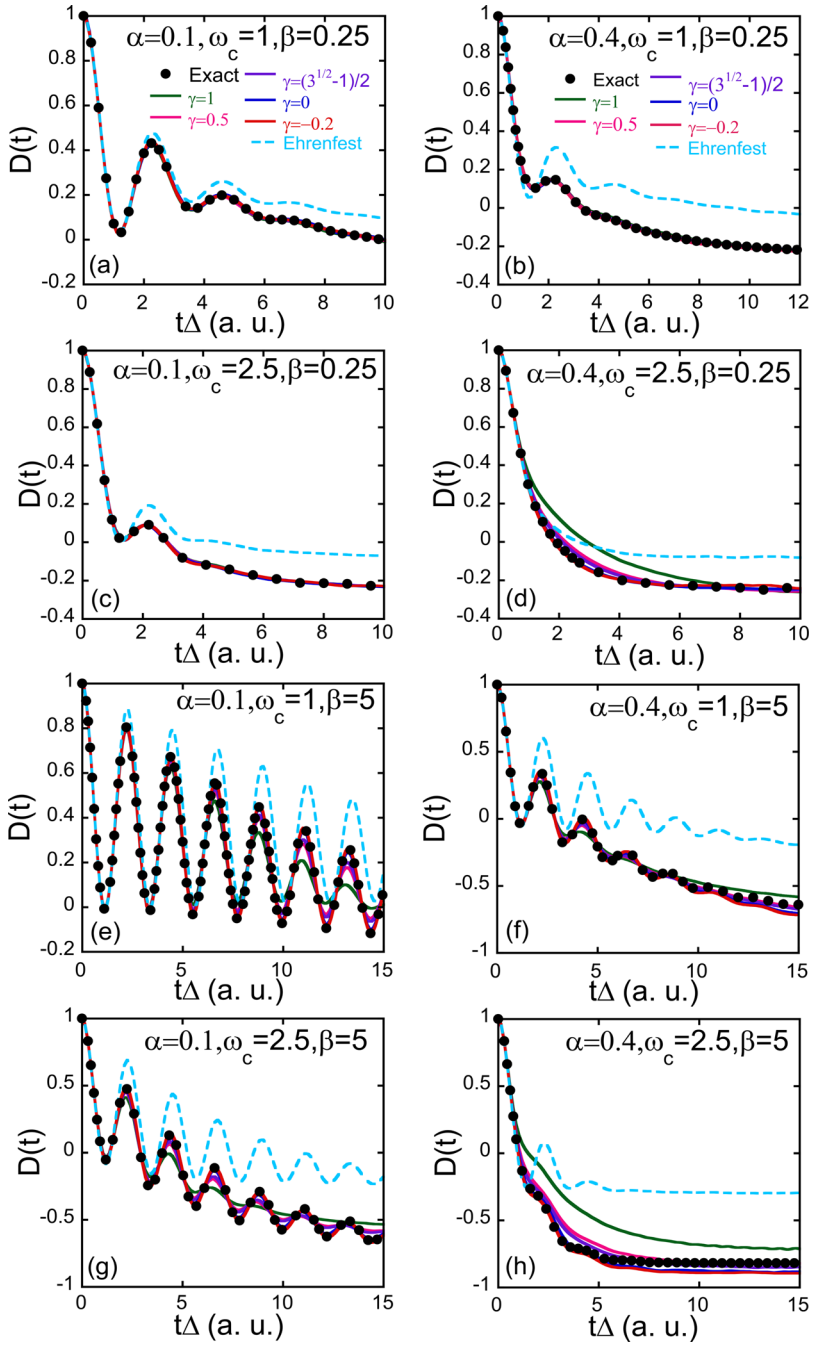

Figure 1. Population difference $D(t) = P_{1\leftarrow 1}(t) - P_{2\leftarrow 1}(t)$ of the spin-boson Hamiltonian with the Ohmic bath at finite temperature. The initial state is set to $|1\rangle$. In all eight panels, $\varepsilon = \Delta = 1$. Black solid circles: numerically exact results in (a), (d), and (e−h) from eHEOM; those in (c) and (d) are from SLNE. Cyan dashed lines: Ehrenfest dynamics. Olive, magenta, purple, blue, and red solid lines: eCMM approach with $\gamma = 1$, 0.5, $(\sqrt{3} - 1)/2$, 0, and −0.2, respectively.

$$P_{m\leftarrow n}(t) = \mathrm{Tr}[\hat{\rho}_{\mathrm{nuc}}|n\rangle\langle n|e^{i\hat{H}t/\hbar}|m\rangle\langle m|e^{-i\hat{H}t/\hbar}] \tag{19}$$

Equation 18 leads to the phase space expression of eq 19

$$P_{m\leftarrow n}(t) = \frac{1}{(2\pi\hbar)^N}\int d\mathbf{R}_0\, d\mathbf{P}_0 \int_{S(\mathbf{x}_0,\mathbf{p}_0)} d\boldsymbol{\mu}(\mathbf{x}_0, \mathbf{p}_0)$$
$$\times \left[\frac{1}{2}((x_0^{(n)})^2 + (p_0^{(n)})^2) - \gamma\right]\rho_{\mathrm{W}}^{(\mathrm{nuc})}(\mathbf{R}_0, \mathbf{P}_0)$$
$$\times \left[\frac{1+F}{2(1+F\gamma)^2}((x_t^{(m)})^2 + (p_t^{(m)})^2) - \frac{1-\gamma}{1+F\gamma}\right] \tag{20}$$

where $\gamma \in (-1/F, \infty)$ and $\rho_{\mathrm{W}}^{(\mathrm{nuc})}(\mathbf{R}_0, \mathbf{P}_0)$ is the Wigner function for $\hat{\rho}_{\mathrm{nuc}}$. We emphasize that there exists only a single value for the ZPE parameter, γ, in the whole mapping scheme in the paper. That is, the ZPE parameter, γ, of the mapping Hamiltonian (eq 2 or 3) is the same as that of the constraint space (eq 4) as well as that employed in the expression of the time correlation function of nonadiabatic dynamics (eq 15 or 18).

It is worth mentioning that, independent of our work,[15,17] in the symmetrical quasiclassical Meyer−Miller (SQC/MM) approach[18] where the ZPE parameter in the Meyer−Miller Hamiltonian is modified on a per trajectory basis, a constraint of the classical actions has been considered such that the original

https://dx.doi.org/10.1021/acs.jpclett.1c00232
J. Phys. Chem. Lett. 2021, 12, 2496−2501

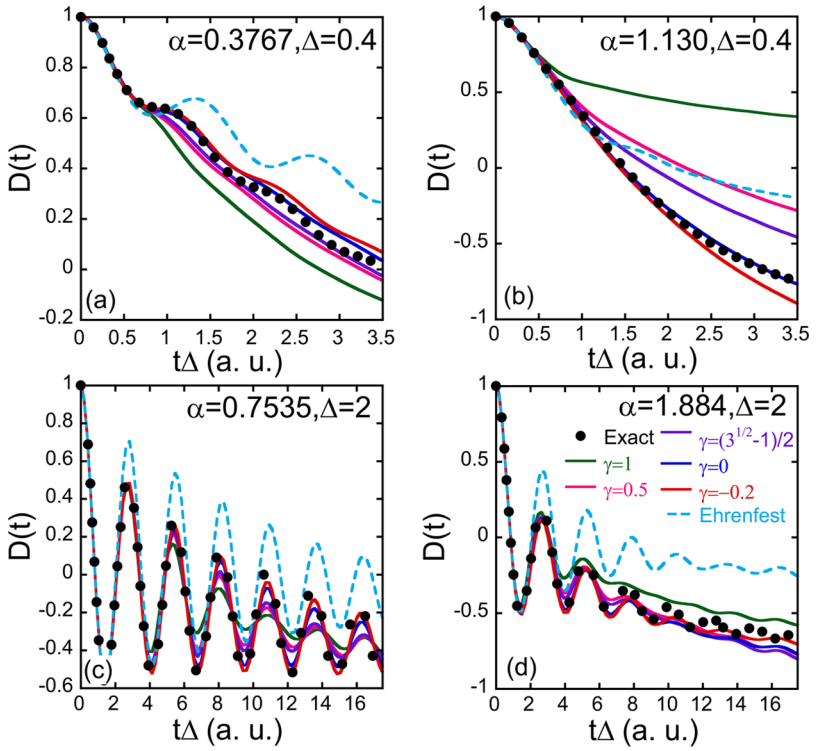

Figure 2. Population difference of the spin-boson Hamiltonian with the Ohmic bath at zero temperature. The initial state is set to $|1\rangle$. In all four panels, $\omega_c = 1.0618$ and $\varepsilon = 1$. The other parameters are (a) $\{\alpha = 0.3767, \Delta = 0.4\}$, (b) $\{\alpha = 1.130, \Delta = 0.4\}$, (c) $\{\alpha = 0.7535, \Delta = 2\}$, and (d) $\{\alpha = 1.884, \Delta = 2\}$. The legend is the same as that in Figure 1, except exact results are produced by ML-MCTDH in ref 29.

Meyer−Miller Hamiltonian (eq 2) is consistent with the typically used symmetrized form of the Hamiltonian. A generalized triangle windowing scheme is used for the initial and final conditions in the SQC/MM approach.[18] It will be interesting to determine whether a rigorous derivation for this trajectory-adjusted ZPE parameter approach is possible and whether the modification strategy on a per trajectory basis can be useful in our exact unified formulation.

Consider the spin-boson model that describes a two-state system coupled with a bosonic bath environment.[19] Such a prototype model in theoretical physics and chemistry includes key aspects of condensed-phase nonadiabatic quantum systems.[19−22] Its Hamiltonian operator reads

$$\hat{H} = \varepsilon\hat{\sigma}_z + \Delta\hat{\sigma}_x + \left(\sum_j c_j\hat{R}_j\right)\hat{\sigma}_z + \sum_j \frac{1}{2}(\hat{P}_j^2 + \omega_j^2\hat{R}_j^2) \tag{21}$$

where $\hat{\sigma}_x$ and $\hat{\sigma}_z$ are Pauli matrices in the x and z directions, respectively, ε represents the detuning between states $|1\rangle$ and $|2\rangle$, Δ denotes the tunneling amplitude, and $\{\hat{R}_j, \hat{P}_j\}$ are the mass-weighted position and momentum operators of the jth bath oscillator, respectively. Frequencies and coupling strengths $\{\omega_j, c_j\}$ are sampled from such as the Ohmic spectral density $J(\omega) = \frac{\pi}{2}\alpha\omega e^{-\omega/\omega_c}$, where α is the Kondo parameter and ω_c the cutoff frequency. The continuous spectral density is discretized into 300 effective bath modes to achieve full convergence. (See the Supporting Information for more details.)

The two-state system is assumed to be initially excited in state $|1\rangle$ with no correlation with the bosonic bath (i.e., the initial density is $|1\rangle\langle 1|\otimes e^{-\beta\hat{H}_b}/Z_b$, where $\hat{H}_b = \sum_j \frac{1}{2}(\hat{P}_j^2 + \omega_j^2\hat{R}_j^2)$ stands for the bare bath Hamiltonian and $Z_b = \mathrm{Tr}_n[e^{-\beta\hat{H}_b}]$ represents the partition function for the bath). While the initial distribution for the nuclear phase space is generated from the Wigner function of $e^{-\beta\hat{H}_b}/Z_b$, that for the electronic Cartesian phase space is uniformly sampled on constraint space $S(\mathbf{x}_0, \mathbf{p}_0)$. The difference from the population of state $|1\rangle$ to that of state $|2\rangle$ (i.e., $D(t) = P_{1\leftarrow 1}(t) - P_{2\leftarrow 1}(t)$) can be evaluated from eq 20. We focus on more challenging asymmetric cases where Ehrenfest's mean field dynamics performs poorly. For fair comparison, the initial condition for the nuclear DOFs in the mean field dynamics is also sampled from the Wigner function of $e^{-\beta\hat{H}_b}/Z_b$, but the initial condition for the electronic DOFs for the two-state system is sampled from $((x^{(1)})^2 + (p^{(1)})^2)/2 = 1$ and $((x^{(2)})^2 + (p^{(2)})^2)/2 = 0$ as conventional Ehrenfest dynamics does. Five values for the ZPE parameter ($\gamma = -0.2$, 0, $(\sqrt{3} - 1)/2$, 0.5, and 1) are used for the eCMM approach for demonstration. Numerical simulations employ an ensemble of 10^5−10^6 trajectories for convergence. Parameters for all examples of the spin-boson model are presented in atomic units (a.u.'s). For comparison, numerically exact results are obtained from the extended hierarchical equations of motion (eHEOM),[23−30] stochastic Liouville−von Neumann equation (SLNE),[31,32] and multilayer multiconfiguration time-dependent Hartree (ML-MCTDH).[33]

Figure 1 presents $D(t)$ for finite bath temperatures. The parameters range from high to low temperatures, from adiabatic to nonadiabatic domains, and from weak to strong system−bath coupling strengths. On the boundary of the adiabatic and nonadiabatic regions ($\omega_c = \Delta$) and in the high-temperature region ($\beta\Delta = 0.25$) the performance of eCMM is insensitive to the value for γ (regardless of whether the ZPE parameter is negative or positive), of which the results perfectly match the exact data (Figure 1a,b). Figure 1c,d lies in the deeper nonadiabatic domain ($\omega_c = 2.5\Delta$) with a relatively high

https://dx.doi.org/10.1021/acs.jpclett.1c00232
J. Phys. Chem. Lett. 2021, 12, 2496−2501

temperature ($\beta\Delta = 0.25$). All five values for γ lead to nearly the same eCMM results that are almost identical to the exact data when the system−bath coupling ($\alpha = 0.1$) is relatively weak (Figure 1c). As the system−bath coupling becomes stronger ($\alpha = 0.4$), $\gamma = -0.2$ or 0 performs the best to describe the exact overdamped dynamics behavior, $\gamma = (\sqrt{3} - 1)/2$ or 0.5 is slightly worse but produces results close to the exact ones, and $\gamma = 1$ exhibits a significant deviation (Figure 1d). Figure 1e,f demonstrates low-temperature ($\beta\Delta = 5$) cases on the boundary of the adiabatic and nonadiabatic regions ($\omega_c = \Delta$). In the weak dissipation case ($\alpha = 0.1$) of Figure 1e, the underdamped oscillation is captured quite well by either $\gamma = -0.2$ or 0 in the whole range of $t\Delta$. The results produced by $\gamma = (\sqrt{3} - 1)/2$ or 0.5 deviate slightly from the exact data after $t\Delta = 5$, while $\gamma = 1$ considerably underestimates the oscillation amplitude. In the stronger dissipation case ($\alpha = 0.4$) of Figure 1f, $\gamma = 1$ shows a more noticeable deviation as the time, $t\Delta$, increases, while the overall dynamic behavior is well reproduced by all four other values for γ. Figure 1g,h falls in the nonadiabatic domain ($\omega_c = 2.5\Delta$) with a low temperature ($\beta\Delta = 5$). In the weak dissipation case in Figure 1g, while $\gamma = -0.2$ or 0 is able to faithfully depict the distinct underdamped behavior in the exact time evolution of $D(t)$, the eCMM approach performs progressively worse in reproducing the long-time oscillation as the value of the ZPE parameter increases in the positive region. For example, $\gamma = 1$ suffers a significant underestimation of the amplitude of oscillation after $t\Delta = 5$. Figure 1h demonstrates the strong dissipation case instead. All values for γ perform well for a short time before $t\Delta = 1$. Three typical categories of results are observed for a longer time. $\gamma = -0.2$ and 0 show the best performance during $t\Delta = 1-6$ but have a slight deviation from the asymptotic limit after $t\Delta = 6$, $\gamma = (\sqrt{3} - 1)/2$ and 0.5 yield good estimations for the long-time equilibrium, and $\gamma = 1$ predicts a slower decay rate and exhibits a large deviation after $t\Delta = 1$, which performs substantially differently from the four other values.

Quantum dynamics of the dissipative two-state system at zero temperature is theoretically much more demanding.[19] Numerical methods for the spin-boson model at zero temperature often have severe slow convergence problems.[21,29,34] Figure 2 shows $D(t)$ for the four asymmetric spin-boson models with the Ohmic bath at zero temperature where exact benchmark results are available.[29] In the deeper nonadiabatic region ($\omega_c = 2.65\Delta$) as shown in Figure 2a,b, $\gamma = -0.2$ and 0 faithfully capture most dynamic behaviors, $\gamma = (\sqrt{3} - 1)/2$ and 0.5 lose the noticeable oscillation details in panel (a) and cause considerable deviation from the exact data in panel (b), while $\gamma = 1$ demonstrates overall poor performance (except at short time) in both cases. In Figure 2c,d, the tunneling amplitude of the spin-boson model ($\Delta = 2$) is increased by a factor of 5 in comparison to that in Figure 2a,b. $\gamma = -0.2$ demonstrates the best performance in reproducing the exact data, especially for the amplitude of dynamic oscillation in either case. The results of $\gamma = 0$ are very close to but slightly worse than those of $\gamma = -0.2$. As the positive value of the ZPE parameter becomes greater, the eCMM results increasingly deviate from the exact data.

In all eCMM applications (with the Meyer−Miller mapping Hamiltonian) for the typical examples of the spin-boson model shown in the main text as well as in the Supporting Information, the negative ZPE parameter (e.g., $\gamma = -0.2$) practically faithfully depicts the dynamic oscillation behavior as well as the asymptotic long-time equilibrium, yielding reasonably accurate results in comparison to conventional positive ZPE parameters. In practice, the numerical performance is relatively insensitive to γ in domain $(-1/F, 1/2]$ for finite temperature spin-boson systems. It is expected that $\gamma \in (-1/F, 1/2]$ may work reasonably well for other complex molecular systems.

In summary, a negative ZPE parameter is indeed possible and can be reasonably good for the Meyer−Miller mapping model for nonadiabatic molecular dynamics because the constraint implied in the kinetic energy term, $\mathbf{P}^T\mathbf{M}^{-1}\mathbf{P}/2$, in the mapping Hamiltonian requests only $\gamma \in (-1/F, \infty)$. When such a constraint is applied, we establish a novel and general formulation for constructing exact mapping models in the Cartesian phase space (for the electronic DOFs). Although the formulation is in principle exact irrespective of the meaningful value of γ, because the nuclear DOFs often cannot be treated in an exact fashion for general nonadiabatic systems, the performance of an approximated quantum dynamics method depends on the choice of the ZPE parameter. Although the dependence of γ is relatively weak in many cases, it can become distinct in demanding regions (e.g., at low or zero temperature in condensed-phase systems). More insight will be warranted in the future to develop a novel strategy in the mapping formulation, which makes the numerical performance of practical nonadiabatic methods much less sensitive to the ZPE parameter, γ.

■ ASSOCIATED CONTENT

Supporting Information

The Supporting Information is available free of charge at https://pubs.acs.org/doi/10.1021/acs.jpclett.1c00232.

Kernel and inverse kernel in a unified mapping framework in quantum mechanics; bath mode discretization; and numerical results for additional typical spin-boson models (PDF)

■ AUTHOR INFORMATION

Corresponding Author

Jian Liu − *Beijing National Laboratory for Molecular Sciences, Institute of Theoretical and Computational Chemistry, College of Chemistry and Molecular Engineering, Peking University, Beijing 100871, China;* orcid.org/0000-0002-2906-5858; Email: jianliupku@pku.edu.cn

Authors

Xin He − *Beijing National Laboratory for Molecular Sciences, Institute of Theoretical and Computational Chemistry, College of Chemistry and Molecular Engineering, Peking University, Beijing 100871, China;* orcid.org/0000-0002-5189-7204

Zhihao Gong − *Beijing National Laboratory for Molecular Sciences, Institute of Theoretical and Computational Chemistry, College of Chemistry and Molecular Engineering, Peking University, Beijing 100871, China;* orcid.org/0000-0002-9643-633X

Baihua Wu − *Beijing National Laboratory for Molecular Sciences, Institute of Theoretical and Computational Chemistry, College of Chemistry and Molecular Engineering, Peking University, Beijing 100871, China;* orcid.org/0000-0002-1256-6859

Complete contact information is available at: https://pubs.acs.org/10.1021/acs.jpclett.1c00232

https://dx.doi.org/10.1021/acs.jpclett.1c00232
J. Phys. Chem. Lett. 2021, 12, 2496−2501

Author Contributions

†X.H. and Z.G. contributed equally.

Notes

The authors declare no competing financial interest.

■ ACKNOWLEDGMENTS

This work was supported by the National Natural Science Foundation of China (NSFC) (grant no. 21961142017) and by the Ministry of Science and Technology of China (MOST) (grant no. 2017YFA0204901). We acknowledge the High-Performance Computing Platform of Peking University, Beijng PARATERA Tech CO., Ltd., and the Guangzhou Supercomputer Center for providing computational resources. We thank Qianlong Wang and Jianlan Wu for providing the eHEOM results in Figure 1a,b,g,h (in the main text), Figure S1 and Figure S2b,c (in the Supporting Information).

■ REFERENCES

(1) Domcke, W.; Yarkony, D. R.; Koppel, H. *Conical Intersections: Theory, Computation and Experiment*; World Scientific: Singapore, 2010.
(2) Martinez, T. J. Physical Chemistry Seaming Is Believing. *Nature* **2010**, *467*, 412−413.
(3) Long, R.; Prezhdo, O. V.; Fang, W. Nonadiabatic Charge Dynamics in Novel Solar Cell Materials. *Wiley Interdisciplinary Reviews-Computational Molecular Science* **2017**, *7*, e1305.
(4) Meyer, H.-D.; Miller, W. H. A Classical Analog for Electronic Degrees of Freedom in Nonadiabatic Collision Processes. *J. Chem. Phys.* **1979**, *70*, 3214−3223.
(5) Sun, X.; Wang, H. B.; Miller, W. H. Semiclassical Theory of Electronically Nonadiabatic Dynamics: Results of a Linearized Approximation to the Initial Value Representation. *J. Chem. Phys.* **1998**, *109*, 7064−7074.
(6) Cotton, S. J.; Miller, W. H. A New Symmetrical Quasi-Classical Model for Electronically Non-Adiabatic Processes: Application to the Case of Weak Non-Adiabatic Coupling. *J. Chem. Phys.* **2016**, *145*, 144108.
(7) Miller, W. H.; Cotton, S. J. Classical Molecular Dynamics Simulation of Electronically Non-Adiabatic Processes. *Faraday Discuss.* **2016**, *195*, 9−30.
(8) Cotton, S. J.; Miller, W. H. A Symmetrical Quasi-Classical Windowing Model for the Molecular Dynamics Treatment of Non-Adiabatic Processes Involving Many Electronic States. *J. Chem. Phys.* **2019**, *150*, 104101.
(9) Stock, G.; Thoss, M. Semiclassical Description of Nonadiabatic Quantum Dynamics. *Phys. Rev. Lett.* **1997**, *78*, 578−581.
(10) Muller, U.; Stock, G. Flow of Zero-Point Energy and Exploration of Phase Space in Classical Simulations of Quantum Relaxation Dynamics. II. Application to Nonadiabatic Processes. *J. Chem. Phys.* **1999**, *111*, 77−88.
(11) Golosov, A. A.; Reichman, D. R. Classical Mapping Approaches for Nonadiabatic Dynamics: Short Time Analysis. *J. Chem. Phys.* **2001**, *114*, 1065−1074.
(12) Kananenka, A. A.; Hsieh, C. Y.; Cao, J. S.; Geva, E. Nonadiabatic Dynamics Via the Symmetrical Quasi-Classical Method in the Presence of Anharmonicity. *J. Phys. Chem. Lett.* **2018**, *9*, 319−326.
(13) Gao, X.; Geva, E. Improving the Accuracy of Quasiclassical Mapping Hamiltonian Methods by Treating the Window Function Width as an Adjustable Parameter. *J. Phys. Chem. A* **2020**, *124*, 11006−11016.
(14) Xie, Y.; Zheng, J.; Lan, Z. Performance Evaluation of the Symmetrical Quasi-Classical Dynamics Method Based on Meyer-Miller Mapping Hamiltonian in the Treatment of Site-Exciton Models. *J. Chem. Phys.* **2018**, *149*, 174105.
(15) He, X.; Liu, J. A New Perspective for Nonadiabatic Dynamics with Phase Space Mapping Models. *J. Chem. Phys.* **2019**, *151*, 024105.
(16) Runeson, J. E.; Richardson, J. O. Spin-Mapping Approach for Nonadiabatic Molecular Dynamics. *J. Chem. Phys.* **2019**, *151*, 044119.
(17) Liu, J. A Unified Theoretical Framework for Mapping Models for the Multi-State Hamiltonian. *J. Chem. Phys.* **2016**, *145*, 204105.
(18) Cotton, S. J.; Miller, W. H. Trajectory-Adjusted Electronic Zero Point Energy in Classical Meyer-Miller Vibronic Dynamics: Symmetrical Quasiclassical Application to Photodissociation. *J. Chem. Phys.* **2019**, *150*, 194110.
(19) Leggett, A. J.; Chakravarty, S.; Dorsey, A. T.; Fisher, M. P. A.; Garg, A.; Zwerger, M. Dynamics of the Dissipative Two-State System. *Rev. Mod. Phys.* **1987**, *59*, 1−85.
(20) Topaler, M.; Makri, N. Path Integral Calculation of Quantum Nonadiabatic Rates in Model Condensed Phase Reactions. *J. Phys. Chem.* **1996**, *100*, 4430−4436.
(21) Wang, H. B.; Thoss, M. From Coherent Motion to Localization: Dynamics of the Spin-Boson Model at Zero Temperature. *New J. Phys.* **2008**, *10*, 115005.
(22) Wang, Q. L.; Gong, Z. H.; Duan, C. R.; Tang, Z. F.; Wu, J. L. Dynamical Scaling in the Ohmic Spin-Boson Model Studied by Extended Hierarchical Equations of Motion. *J. Chem. Phys.* **2019**, *150*, 084114.
(23) Tanimura, Y.; Kubo, R. Time Evolution of a Quantum System in Contact with a Nearly Gaussian-Markoffian Noise Bath. *J. Phys. Soc. Jpn.* **1989**, *58*, 101−114.
(24) Tanimura, Y. Reduced Hierarchical Equations of Motion in Real and Imaginary Time: Correlated Initial States and Thermodynamic Quantities. *J. Chem. Phys.* **2014**, *141*, 044114.
(25) Yan, Y. A.; Yang, F.; Liu, Y.; Shao, J. S. Hierarchical Approach Based on Stochastic Decoupling to Dissipative Systems. *Chem. Phys. Lett.* **2004**, *395*, 216−221.
(26) Shao, J. S. Stochastic Description of Quantum Open Systems: Formal Solution and Strong Dissipation Limit. *Chem. Phys.* **2006**, *322*, 187−192.
(27) Xu, R. X.; Cui, P.; Li, X. Q.; Mo, Y.; Yan, Y. J. Exact Quantum Master Equation Via the Calculus on Path Integrals. *J. Chem. Phys.* **2005**, *122*, 041103.
(28) Moix, J. M.; Cao, J. S. A Hybrid Stochastic Hierarchy Equations of Motion Approach to Treat the Low Temperature Dynamics of Non-Markovian Open Quantum Systems. *J. Chem. Phys.* **2013**, *139*, 134106.
(29) Tang, Z.; Ouyang, X.; Gong, Z.; Wang, H.; Wu, J. Extended Hierarchy Equation of Motion for the Spin-Boson Model. *J. Chem. Phys.* **2015**, *143*, 224112.
(30) Duan, C.; Wang, Q.; Tang, Z.; Wu, J. The Study of an Extended Hierarchy Equation of Motion in the Spin-Boson Model: The Cutoff Function of the Sub-Ohmic Spectral Density. *J. Chem. Phys.* **2017**, *147*, 164112.
(31) Stockburger, J. T.; Mak, C. H. Dynamical Simulation of Current Fluctuations in a Dissipative Two-State System. *Phys. Rev. Lett.* **1998**, *80*, 2657−2660.
(32) Imai, H.; Ohtsuki, Y.; Kono, H. Application of Stochastic Liouville-Von Neumann Equation to Electronic Energy Transfer in FMO Complex. *Chem. Phys.* **2015**, *446*, 134−141.
(33) Wang, H. B.; Thoss, M. Multilayer Formulation of the Multiconfiguration Time-Dependent Hartree Theory. *J. Chem. Phys.* **2003**, *119*, 1289−1299.
(34) Wang, H. B.; Thoss, M. From Coherent Motion to Localization: II. Dynamics of the Spin-Boson Model with Sub-Ohmic Spectral Density at Zero Temperature. *Chem. Phys.* **2010**, *370*, 78−86.

https://dx.doi.org/10.1021/acs.jpclett.1c00232
J. Phys. Chem. Lett. 2021, 12, 2496−2501